NJC

Accepted Manuscript

ROYAL SOCIETY OF CHEMISTRY

www.rsc.org/njc

Journal Name

ARTICLE

Towards Designed Synthesis of Metallic Nanoparticles in Polyols - Elucidation of the Redox Scheme in Cobalt-Ethylene Glycol System

Kazuma Takahashi,[a] Shun Yokoyama,[b] Takatoshi Matsumoto,[c] Jhon L. Cuya Huaman,[a] Hisashi Kaneko,[a] Jean-Yves Piquemal,[d] Hiroshi Miyamura[b] and Jeyadevan Balachandran[a],*

The polyol process has been used to synthesize metal and alloy nanoparticles over a couple of decades. Its potential has been demonstrated through the synthesis of metallic nanoparticles with various sizes and shapes. However, though one of the roles of polyol is to be a reducing agent, researches related to the investigation of the redox reaction mechanism have been scarce. In this study, we report the results of a detailed study undertaken to investigate the polyol oxidation and metal reduction for the cobalt(II)−ethylene glycol with the possible addition of a base (Na) in the system using several physico-chemical techniques such as NMR, FT-IR, ESI-TOFMS and XRD. The results suggested that in the reduction reaction, ethylene glycol first reacts with the base to produce the ethylene glycol monoanion, here in after denoted as EG^-. This reaction not only occurs between ethylene glycol and the base, but also occurs with Co^{2+} species. In such a case, the formation of Co alkoxide and subsequent reduction could progress even in the presence of a weak base such as acetate ion or any other solvent that has lone pair of electrons such as oxygen in ether. On the other hand, in the case of oxidation of ethylene glycol, first the base attacks one of the two α proton in Co alkoxide and along with the electrons transfer to Co^{2+}, ethylene glycol get oxidized to aldehyde. Then, the aldehyde thus formed undergoes bond exchange with the neighboring coordinated ethylene glycol and an ester is formed. The above steps are repeated and the hydrogen atoms coordinated with Co get detached with the evolution of hydrogen gas, while ethylene glycol is oxidized to polyglycolic acid. The analytical techniques and the results obtained in this study could be used to enhance the properties of metals and alloys nanoparticles synthesized using the polyol process.

1 Introduction

Nano-sized metallic and alloy materials have been proved to exhibit properties that can significantly differ from those of their bulk counterparts due to the increase in the ratio of surface to core atoms and quantum effects. For instance, steep drops in melting points or increases in catalytic activity for structure-sensitive reactions have been reported for reduced particle sizes.[1,2] On the other hand, the influence on electrical and thermal properties due to quantum effects have made potential application in engineering and biomedicine possible.[3] The bottom-up approaches have been successfully carried out to acquire metallic materials in the nanoscale regime and are mainly divided into gas phase and liquid phase reactions. Several liquid phase synthesis techniques have been developed for the preparation of metallic nanoparticles. Among them, two methods have been widely used: the organometallic pathway and the polyalcohol route. The organometallic chemistry route consists of the reduction of an organometallic precursor in a non-polar solvent, generally using hydrogen gas as reducing agent.[4] On the other hand; in the polyol/alcohol route, straight chain alcohols and polyalcohols are being used as reducing agents for the preparation of metal nanoparticles,[5-12] which also provide a reducing atmosphere and protects the nanoparticles from oxidation. This has led to the synthesis of not only various precious metals, but also some transition metals such as nickel and copper.[6,13] However, a serious impediment lies in the fact that the polarity of straight chain alcohol is relatively low compared to water and the solubility of metal salts is limited. On the other hand, to improve the reducing potential, alcohols with long chains displaying high boiling points are preferred. But this may lead to further reduction in their polarity and solubility, which could be detrimental for large-scale production. However, this is a very useful technique to obtain particles with unique properties.

On the other hand, polyalcohols, known as polyols, have numerous hydroxyl groups compared to straight chain alcohols and their reduction ability, polarity as well as their boiling point are high. As a result, the solubility of metal salts is higher in polyols than in mono-alcohols. In 1989, Fiévet et al. reported the preparation of metal nanoparticles via the polyol process. In this method, the polyalcohol acts as a solvent, a reducing agent and a protecting agent.[14-16]

[a] Department of Materials Science, The University of Shiga Prefecture, Hikone 522-8533, Japan. Email: Jeyadevan.b@mat.usp.ac.jp
[b] Graduate School of Environmental Studies, Tohoku University, Sendai 980-8579, Japan.
[c] Institute of Multidisciplinary Research, Tohoku University, Sendai 980-8577, Japan.
[d] Université Paris Diderot, Sorbonne Paris Cité, ITODYS, CNRS UMR 7086, Paris, France.
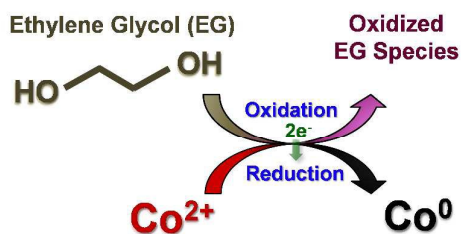
Figure 1. Schematic illustration of redox reaction during the synthesis of metallic cobalt using ethylene glycol as reducing agent.

Figure 2. Formation schemes of cobalt alkoxide and metallic cobalt in (a) EG-CoCl$_2$-NaOH and (b) EG- Co(OAc)$_2$ systems.

Subsequently, this led to the successful syntheses of various transition metals including iron and their alloys with reasonable ease.[17-21] Furthermore, capitalizing on the solvent and surfactant properties of polyalcohol, the syntheses of various metal oxides with enhanced physical properties have also been demonstrated.[22-25] In the context of the synthesis of metals and alloy nanoparticles, the polyol process possess many excellent features compared to other non-aqueous techniques such as thermal decomposition, etc. and can be considered as a practical solution to nanomaterial synthesis. However, in order to exploit the full potential of this process, some work is necessary in order to obtain a better understanding on the reaction mechanism and particularly on the reduction/oxidation reaction schemes accounting for the formation of the metallic nanoparticles.

During the course of the reaction, polyol molecules reduce metal ions and at the same time, undergo oxidation. For example, if we consider the synthesis of metallic cobalt using ethylene glycol (EG), the redox reaction can be illustrated schematically as shown in Figure 1.

Though the reduction of metal ions and oxidation of polyol molecules are presumed during the formation of metal particles, detailed electron transfer mechanism has not been elucidated fully. Though the influence of metal salts, additives such as hydroxyl ions, and the formation of the intermediate products during the reduction of Co^{2+} to Co^0 has been studied in the past,[14,18-23] the diverse behaviours of cobalt salts in EG are yet to be explained. For example, in the EG−CoCl$_2$ system, metallic Co particles are not obtained even if the system is heated up to the boiling point of EG and reacted for more than 24 h. However, the formation of metallic Co via the reduction of the Co alkoxide intermediate has been reported in the cases of EG−Co(OAc)$_2$ and EG−CoCl$_2$−NaOH system.[26] It is well known that the alcohol can be considered as a weak base as well as weak acid[27] and become a weak acid by donating the proton to water in dilute aqueous solution. However, in the case of ethylene glycol, there are two hydroxyl groups and the active species that contribute to the dissolution and reduction of metal ions have not been discussed in the past.

Only recently, theoretical and experimental investigations to understand the dissolution and reduction of cobalt ions in the polyol process using ethylene glycol was attempted by Matsumoto et al.[28] Out of the two deprotonated states of EG, the monoionic state has been found to contribute to the complex
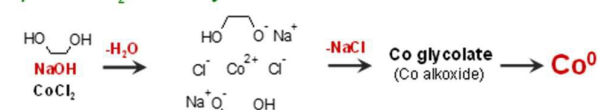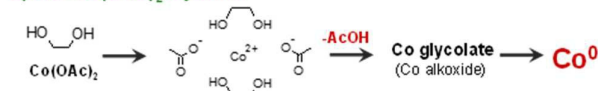
forming reaction as well as reduction reactions during the formation of metallic cobalt from the molecular orbital theory calculations.[28] Though the energy state of dianion of EG has been found to be very high, the probability of their presence in the reaction system is considered low. On the other hand, the monoanionic state of EG is considered stable when the proton in the hydroxyl ion is sandwiched between the two oxygen atoms (*cis* configuration). The energy level of the HOMO associated to this structure is low and so the reactivity with metallic ions. However, when EG is heated close to the boiling temperature, the hydrogen bond is broken and the monoanion of EG attains highly reactive higher energy state (*trans* configuration). Consequently, the strong base generated in the reaction system facilitates the formation of Co glycolate at higher temperature. Thus, in the cases of EG−Co(OAc)$_2$ or EG−CoCl$_2$−NaOH systems, the proton in EG is removed by AcO$^-$ ion or OH$^-$ ion and the active species of EG, EG$^-$ (HOC$_2$H$_4$O$^-$, monoanion) facilitates the formation of Co glycolate, which subsequently get reduced to form metallic cobalt.[19] Furthermore, the structure of Co glycolate has been investigated by Chakroune and Hiyama.[29,30] These reactions in the above two cases are summarized in Figure 2, and in both cases the Co glycolate adopts the Brucite-like structure.[29]

From the above studies, it has been confirmed that in the case of EG−Co^{2+} system, the reduction reaction progresses via the transformation of Co^{2+} to Co glycolate. In other words, it could be inferred that the formation of Co glycolate is a necessary condition for the progression of the reduction reaction. However it has been not studied in detail.[14] Furthermore, the evolution of the metal particles from the intermediate phase or their growth as a function of reaction time has not been analysed in the past.

The redox reaction shown in Fig. 2 can be explained only by elucidating the coordinated structures of Co formed during the reaction. However in the proposed reaction scheme, the electron transfer during the reduction of Co glycolate to metallic cobalt has not been described. And also, in order to fully understand the electron transfers of the sequence of redox reactions, not only the reduction reaction of Co^{2+}, but also the oxidation reaction of EG should be clarified. Thus, in the next section, we review the studies carried out to understand the oxidation reaction of EG to date.

New Journal of Chemistry Accepted Manuscript

1.1 Previous study on the oxidation reactions of EG in polyol method

The reduction potential of polyol has been attempted through experimental and quantum chemical calculations and reported to increase with temperature.[31-34] The reaction pathways of the oxidation of polyol and the reduction of metallic ion for the case of $Co(OH)_2$ in EG has been reported over a quarter century ago by Fiévet et al. and this has been widely accepted.[14] According to this reaction, the EG undergoes dehydration and leads to the formation of acetaldehyde (AcH). Then, the AcH reduces Co^{2+} ion and AcH itself undergoes oxidation to form diacetyl as shown in Eq. 1.

$$(1)$$
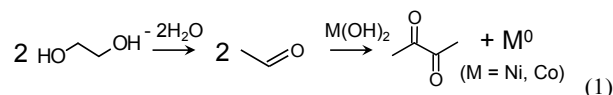
The above reaction has been confirmed using ^1H NMR and the formation of diacetyl has been reported to coincide exactly with the formation of the metallic phase.[14b] It has to be pointed out that the Co particles were prepared by heterogeneous nucleation using pre-formed 3.0 nm sized Pd particles, which may have triggered some organic reactions functioning as a catalayst.[14b]

However, it should be noted that even when AcH was introduced into the EG−Co^{2+} system, the formation of metallic cobalt was not observed and this was believed due to low boiling point of AcH, which is about 20 °C. On the other hand, during the synthesis of transition metals including Co, instead of AcH, a strong base such as NaOH has been introduced as a promoter of the reduction reaction.[15,26,28] However, it should be noted that a substance that contained carbonyl group evolved during the formation of metallic cobalt using EG has been experimentally verified.[26]

Recently an alternative redox reaction has been proposed for systems synthesizing Cu and Ni particles using EG in the presence of hydroxyl ions.[35] The redox reaction consisting of the electron transfers shown in Eq. 2 has been proposed and considered highly valid.[29]

$$(2)$$
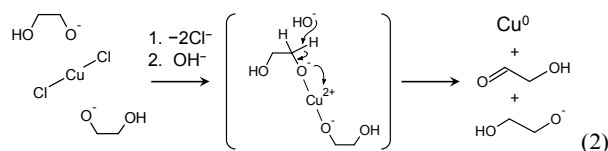
In this reaction, OH^- attacks the proton in the metal glycolate complex and one of the electron pairs in the oxygen atom is transferred to the copper center. This scheme indicates that the divalent metal ion is reduced to zero valent metal atom through the oxidation of the coordinated EG in metal glycolate to glycolaldehyde. However, if EG^- is generated along with zero valent metal, then this reaction could be initiated with a base concentration lesser than the stoichiometric value and reduction reaction should proceed till all the metal ions are reduced. But, this was not the case in reality.

Thus, all these discrepancies observed in the past investigations point that the elucidation of the redox reaction focusing on the oxidation reaction of EG is essential. In this study, we report the results of a detailed investigation carried out to elucidate the redox reaction in Co-EG case using several physicochemical techniques.

2 Experimental

2.1 Materials:

Cobalt salts such as cobalt(II) chloride hexahydrate ($CoCl_2·6H_2O$, 98%), sodium metal, ethylene glycol (HO-CH_2-CH_2-OH, 99.5%), dodecane, methanol, tetradecane, ethylene glycol dibutyl ether and sodium hydroxide (NaOH, 97%) were purchased from Wako Pure Chemicals Ltd., Japan. The commercially available reagents were used without any further purification. To assess the influence of water, anhydrous $CoCl_2$ was used for some experiments. $CoCl_2·6H_2O$ was heated under vacuum at 70 °C till the colour of the powder changed from red to blue. Then, vacuum drying was continued for another extra day to obtain anhydrous $CoCl_2$.

2.2 Sample Preparation:

The basic steps involved in a typical experiment are as follows: 0.1 mol of metal salt is dissolved in 100 mL of EG followed by the addition of either sodium metal or sodium hydroxide. Then, the EG-metal salt or EG-metal salt-sodium metal/sodium hydroxide system is heated to specified temperatures to obtain intermediate products or cobalt metal particles. Samples are recovered by centrifuging the suspensions and washing the precipitates thus obtained with acetone. Then, the products obtained are dried in vacuum at room temperature prior to any further analysis. The preparation methods of some specific samples are given as follows:

a) Preparation of $Co(OH)_2$: 0.1 mol of $CoCl_2·6H_2O$ was dissolved in 100 mL of distilled water in a beaker. In a separate beaker, 0.2 mol of NaOH was dissolved in 100 mL of distilled water. Then, the sodium hydroxide solution was introduced into the already prepared cobalt chloride solution and stirred for 10 minutes at R.T. for the progression of the reaction shown in equation 3. The pink coloured precipitate was recovered using centrifugation and washed with water repeatedly to remove the sodium chloride and other by-products. Then, the sample was washed a couple of times using acetone to facilitate the subsequent vacuum drying process.

$$(Co^{2+})_{aq} + 2OH^- \rightarrow Co(OH)_2 \downarrow \qquad (3)$$
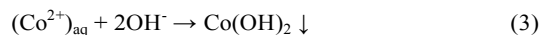
b) Reduction reaction of $Co(OH)_2$ in EG: 10 mmol of $Co(OH)_2$ synthesized in the above experiment and 100 mL of EG were introduced into a 300-mL four-necked separable flask. The suspension was heated to 190 ºC at the rate of 5 ºC/min while stirring at 200 rpm under nitrogen purging (200 mL/min). Then, the suspension was maintained at 190 ºC for 5h. 10 mL of the suspension was withdrawn when the system reached 50

ARTICLE

Journal Name

ºC and 190 ºC and thereafter every 60 min of reaction time. The precipitates obtained during sampling were recovered using centrifugation and washed three times with 20 mL of acetone and vacuum dried. Then, these powders were analysed using XRD.

c) Preparation of EG⁻/EG solution: n mmol (n = 10, 20, 30, 40) of sodium metal was introduced into a 300-mL four-necked flask and 40 mL (0.65 mol) of EG was subsequently introduced. The suspension was heated to 100 ºC at the rate of 5 ºC/min while stirring at 500 rpm under a nitrogen purging to facilitate the reaction between sodium metal and EG as shown in equation 4. When the system was heated under nitrogen purging, hydrogen gas was evolved. Once the dissolution of sodium was confirmed, the solution was cooled to 50 ºC.

$$2HOC_2H_4OH + 2Na \rightarrow 2HOC_2H_4O^- + 2Na^+ + H_2\uparrow \quad (4)$$

d) Preparation of Co glycolate: 0.10 mol of CoCl$_2$ was dissolved in 100 mL of EG, and introduced into the solution containing sodium glycoxide prepared in section (c) and initiated the reaction as shown in equation 5. The suspension was heated to 190 ºC at the rate of 5 ºC/min while stirring at 200 rpm under nitrogen purging (200 mL/min). Then, the suspension was maintained at 190 ºC for 5 min. The pink coloured precipitate was recovered using centrifuging and suction filtering, and was washed with acetone repeatedly to remove the sodium chloride and other by-products. The washed precipitate was vacuum dried.

$$2HOC_2H_4ONa + CoCl_2 \rightarrow Co(OC_2H_4O)\downarrow + 2NaCl + HOC_2H_4OH \quad (5)$$
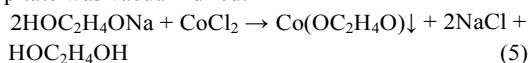
e) Reduction reaction of Co glycolate using aprotic solvents: 10 mmol of Co glycolate was introduced into a 300-mL four-necked separable flask and subsequently 100 mL of either tetradecane or ethylene glycol dibutyl ether was introduced. The suspension was heated under nitrogen flow (200 mL/min) to 190 ºC at the rate of 5 ºC/min while stirring at 200 rpm and maintained at this temperature for 24 h. Then, the suspension was cooled to R.T. and the precipitates obtained with tetradecane and ethylene glycol dibutyl ether solvents were recovered by centrifugation, washed with acetone and vacuum dried.

2. 3 Characterization:

a) Crystal structure analysis: Powder X-ray diffraction (XRD) patterns of the precipitates were carried out using a Panalytical X'pert pro diffractometer (Philips X' Pert-MRD, CuKα (λ =1.5418 Å), operating at 40 kV and 40 mA, generally in the range 2θ = 10º−90º) to identify the Co phases (fcc Co (ICDD 00-015-0806) and hcp Co (ICDD 00-005-0727)) were used to identify.

b) Identification of the organic compound in the liquid: Proton Nuclear Magnetic Resonance (^{1}H NMR) spectroscopy was used to analyze the organic compounds in the liquid samples dissolved in either CDCl$_3$ or D$_2$O. A JEOL LA400 FT-NMR (400 MHz) spectrometer was used. Data of four

consecutive measurements were cumulated for spectral analysis.

c) Identification of functional groups: Fourier Transform Infrared Spectroscopy (FT-IR, Thermo Scientific Nicolet iS5 with ATR attachment) was used to characterize various functional groups present in the organic products using the measurement range of 4000−500 cm^{-1}.

d) Molecular weight analysis of the solvated chemical species: Electrospray Ionization-Time of Flight Mass Spectroscopy (ESI-TOFMS, Bruker Daltonics micrOTOF II) was used to identify chemical species in the liquid phase. Unless stated otherwise, the peaks detected during the measurements are positively charged species. Measurement range is 50−3000 m/z and extra-pure water was used as solvent during measurements. The machine is tuned using 10 mM of formic acid. The spectra are analyzed using the Data-Analysis Version 4.0 SP 1 (Bruker Daltonics).

3 Results and discussion

3.1 Verification of the reduction scheme using Co(OH)$_2$ as precursor:

Co(OH)$_2$ was synthesized as described in 2.2 (a). The crystal structures and morphologies of the products obtained at different reaction times were analyzed using the XRD and SEM and shown in Figure 3.

As it is obvious from Figure 3 (A), at the reaction temperature of 50 ºC, Co(OH)$_2$ remained unreacted. However at 190 ºC, Co(OH)$_2$ transformed to Co glycolate. As the reaction time at 190 ºC was prolonged, the formation of fcc-Co was detected. In addition, Fig. 3 (B) shows the SEM images of layered Co(OH)$_2$ precursor and their progressive transformation to irregular spherical shaped Co particles with an average size of 1 micron at 190 ºC for 3 h of reaction. As in the case of other metal salts,[14,18-23] the formation of the intermediate product, Co glycolate has been confirmed.[14]

When Co(OH)$_2$ was used as Co precursor, the intrinsic basicity of Co(OH)$_2$ seems to be sufficient enough to initiate the redox process. It was proposed that OH⁻ anions originating from the Co precursor deprotonated ethylene glycol to give rise to the formation of monoanion EG⁻, which subsequently helped to generate cobalt glycolate.[28] As it has been already reported, the presence of EG⁻ (monoanion) in the system is indeed required for the dissolution of the Co solid precursor as well as the reduction of Co(II) species. Moreover, the progression of the reduction reaction is inferred to be proportional to the concentration EG⁻.

To verify this proposition, the influence of the ratio between Co^{2+} and EG⁻ was varied and the resultant products were analysed and the results are presented in the next section. To avoid the formation of cobalt hydroxide, metallic sodium was used as the base to generate EG⁻.

3.2 Experimental verification of the influence of EG⁻ concentration on the reduction of Co^{2+}:
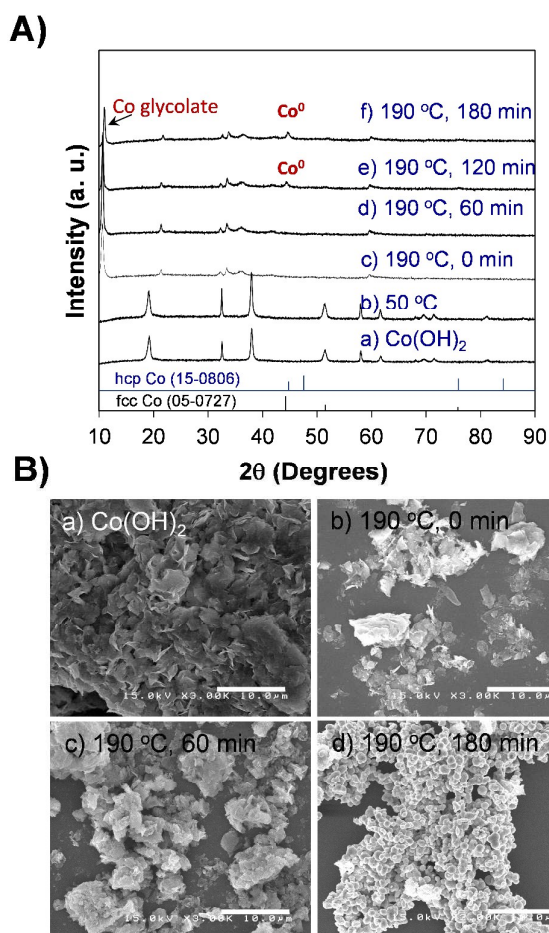
Figure 3. (A) XRD profiles and (B) SEM images of precipitates obtained under different reaction temperatures and time. Scale bar: 10 μ

Figure 4. (A) XRD profiles of precipitates synthesized at 190 °C for 3 h and under different EG⁻ concentrations (amount of Na) in EG using CoCl₂ as the cobalt precursor. (B) SEM images took at different temperatures and reaction times for the case of 40 mmol Na. Scale bar: 1 μm

Solutions with varying EG⁻/EG ratio were prepared by introducing 10, 20, 30 and 40 mmol of metallic sodium into 40 mL of EG. To each of these solutions, 10 mmol of CoCl₂ dissolved in 60 mL of EG was added at R.T and stirred. Subsequently, the solution was heated to 190 ºC at the rate of 5 ºC/min under nitrogen purging and maintained at this temperature for either 3 or 24 h. Then, the reactants were cooled to R.T. and the solid precipitate was recovered by centrifugation, washed with acetone three times and dried. Finally, the XRD profiles of the solid precipitates obtained with different EG⁻ (monoanion) concentrations were compared to evaluate the progression of the reaction. The XRD profiles of the precipitates obtained after reacting at 190 ºC for 3 h are shown in Figure 4.

As seen in Figure 4 (A), the diffraction pattern obtained for the precipitate using 10 mmol of metallic Na did not match with either the known profile of Co glycolate or metallic cobalt (fcc or hcp phase). However, when the concentration of metallic sodium was raised to 20 mmol, the formation of Co glycolate was confirmed. This suggested that a minimum

amount of Na, hence EG⁻, is necessary for the formation of glycolate. And when the concentration of metallic Na was increased to 30 mmol, the precipitation of metallic Co was detected and the amount increased. Further increase was observed when the concentration of metallic Na was raised to 40 mmol.

The above results confirmed that the increase in the concentration of free EG⁻ facilitates the reduction of Co glycolate to metallic cobalt. Consequently, it was revealed that the concentration of the base, EG⁻ promotes the reduction reaction in the CoCl₂−EG−Na system. These results proved that EG⁻ species not only promote the formation of Co glycolate, but also promote its reduction to metallic cobalt. SEM images of the samples synthesized at a metallic Na concentration of 40 mmol are shown in Figure 4 (B). At 120 ºC, the sample was composed of irregular Co glycolate particles with an average size of around 110 nm. However, at higher reaction temperature, the particles agglomerated and grew into big aggregates of Co metal.

Figure 5 (A) shows the XRD profiles of the precipitate obtained after a reaction time of 24 h for different

A)

B)
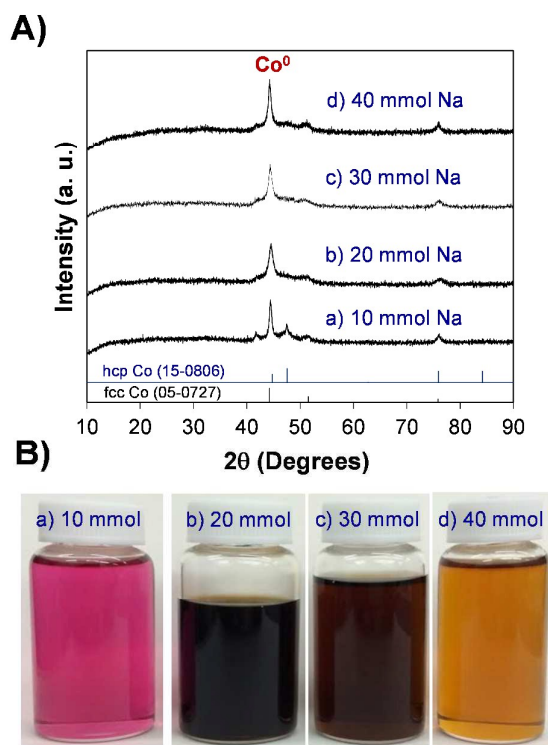
Figure 5. (A) XRD profiles of precipitates synthesized at 190 ^{o}C for 24 h and under different EG$^-$ concentrations (amount of Na) in EG using CoCl$_2$ as the cobalt precursor. (B) Photographs of the supernatants are also observed.

A)

B)

C)

Figure 6. A) XRD profiles of Co alkoxide and precipitates synthesized at 190 ^{o}C for 24 h in (a) tetradecane and (b) ethylene glycol dibutyl ether. B) Schematic illustration of the initial redox reaction for Co alkoxide. C) SEM images of samples synthesized in (a) ethylene glycol and (b) ethylene glycol dibutyl ether. Scale bar: 5 μm.

concentrations of metallic Na. For prolonged reaction time, Co^{2+} underwent reduction to metallic Co irrespective of the concentration of metallic Na. This suggests that if reacted for prolonged period, the Co^{2+} could be reduced to metallic Co even without the use of the strong base such as EG$^-$. However, it was observed that all the Co^{2+} species were not reduced and the yield of metallic cobalt depended on the amount of metallic Na. The yield of metallic cobalt synthesized at 190 ^{o}C for 24 h were 37.2, 87.3, 75.2 and 78.9 % for the metallic Na concentrations of 10, 20, 30 and 40 mmol, respectively. For the formation of Co glycolate, twice the amount of EG$^-$ in reference to the concentration of cobalt ion is required. Thus 10 mmol of Co ion could not be converted to Co glycolate with EG$^-$ generated using less than 20 mmol of metallic Na.

Unconverted Co^{2+} ions remained in the solution and were removed during washing. The photographs of the supernatant solutions after the reaction are shown in Figure 5 (B). The colour of the solution obtained by reacting 10 mmol of Na was pink due to the presence of strong base that facilitated the formation of Co glycolate. However, strong base may not be necessary for the reduction of Co glycolate to metallic Co. In the CoCl$_2$−EG−Na system, after total consumption of Na and generation of the EG$^-$, only the lone-pair electrons of oxygen (Lewis base) in either EG$^-$ or EG remain. Thus, once the formation of Co glycolate is realized, the reduction reaction may progress even with weak base such as EG. However, the progression of the reduction of Co^{2+} through the thermal

decomposition of Co glycolate cannot be ruled out. Thus to determine the true nature of the reduction reaction, experiments were designed with aprotic and protogenic solvents and the results are reported below.

3.3 Verification of the reduction scheme of Co glycolate using aprotic and protogenic solvents:

To verify the reduction scheme, the influence of the solvent structure on the final product was studied. To prevent the acid-base reaction of the solvent with Co glycolate, reaction was attempted using aprotic solvents. Ethylene glycol dibutyl ether (C$_{10}$H$_{22}$O$_2$) that contains lone pair of electrons and functions as a Lewis base, and tetradecane (C$_{14}$H$_{30}$) that does not contain lone pair of electrons were used. The Co alkoxide synthesized using the experimental scheme described in eq. 5 was introduced into ethylene glycol dibutyl ether and tetradecane separately and heated at 190 ºC for 24 h. Then, the precipitates were recovered and washed with acetone and vacuum dried. The progression of the reduction reaction was monitored by analyzing the precipitates using XRD and SEM (Fig. 6).

As shown in Figure 6 (A), the Co glycolate was not reduced to metallic cobalt when it was heated in tetradecane. However, the formation of metallic Co was detected when ethylene glycol
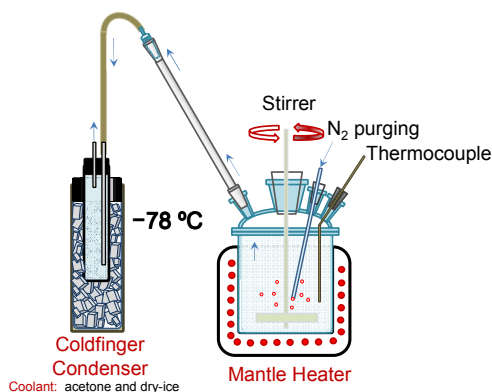
Figure 7. Schematic illustration of the experimental setup used for the collection of low boiling point oxidized species of EG.

Figure 8. ^{1}H NMR spectra of EG, AcH, and samples No. 1, 2, 3, 4a and 4b. Tetramethylsilane (TMS) was used as an internal standard. Inset: ^{1}H-NMR spectrum of EG in D_2O.

dibutyl ether was used as the solvent. The above results confirmed that Co glycolate could be reduced not only by a strong base such as EG$^-$ but also, using a weak base such as ether oxygen. Thus the initial redox reaction of Co glycolate can be schematically represented as shown in Figure 6 (B). However, it should be noted that the reduction reaction would proceed rapidly, when a strong base such as EG$^-$ is used instead of a weak base. Furthermore, progression of the reduction reaction depends on the amount of the base.

The SEM images of Co particles synthesized in ethylene glycol and ethylene glycol dibutyl ether are shown in Figure 6 (C). The particles synthesized in both solvents were nearly spherical in shape with sizes around 360 nm and 610 nm for ethylene glycol and ethylene glycol di butyl ether, respectively. The difference in sizes could be ascribed to the reduction potential of the solvents as well as their capability to adsorb onto the surface of formed particle and subsequently limit their growth.

Though the above reduction scheme has been proposed, it is necessary to investigate the oxidation reaction of EG to elucidate the overall redox reaction mechanism. If the compound formed during the oxidation of EG could be identified, then the validity of the redox reaction proposed in Figure 6 (B) could be verified. Furthermore, the reaction scheme after the attack of Co glycolate by the base could also be identified.

3.4 Elucidation of the oxidation reaction of ethylene glycol:

In this section, the products formed from the oxidation of EG was studied. The experiments discussed below were carried out by heating the reactants to 190 ºC and maintaining at this temperature for 5 h. The experimental setup used is as shown in Figure 7. Since the formation of low boiling point chemical compounds such as acetaldehyde (AcH) and diacetyl have been proposed in the oxidation reaction of EG (Eq.1),[14] the experimental device consisted of a coldfinger condenser tube. The suspension obtained after the reaction was centrifuged to remove the solid precipitate, and the supernatant phase was used for further analyses. Furthermore, to assess the possible formation of oligomers resulting from the condensation of EG$^-$ oxidized species, water and sodium hydroxide were introduced
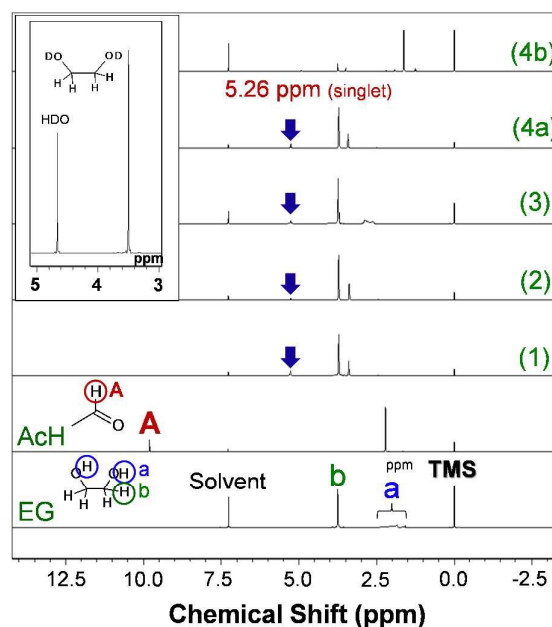
and the reaction mixture was heated at 80 ºC for three days under continuous stirring.

In experiment No. 1, the influence of heating on the structural transformation of EG was studied. In experiment No. 2, the influence of water on the chemical transformation of EG was investigated. In contrast to the above two cases, in experiment No. 3, the conditions appropriate for the reduction of Co^{2+} was used and the EG-oxidized species evolved during the reduction reaction were analysed. In experiment No. 4, the role of Co particles as catalyst was investigated. Finally in experiment No. 5, the concentration of Co^{2+} was set higher than experiment No. 3, expecting larger amount of EG-oxidized species. The samples obtained under the experimental conditions described above were analysed using NMR, FTIR, and ESI-TOFMS. The samples separated from the suspension were named as 1, 2, 3, 4a, 5a. The colour of samples 1, 2, 3 and 4a were pale yellow, colourless, brown and yellow, respectively. Condensed liquid was not obtained in the coldfinger during experiment No. 1, 2, 3 and 5. However, 0.15 g of colourless transparent liquid was collected in experiment No. 4 and named as 4b. The sample obtained by the hydrolysis of 5a is named as 5b and both the samples were dark brown in colour. The identification of the EG-oxidized species generated during the synthesis of metallic Co particles were attempted as given below.

If we assume that AcH is generated during heating and acts as a reducing agent in the system, for 1 mol of Co^{2+} 2 mol of AcH should be generated for the completion of the reduction reaction. In experiment No. 3, Co^{2+} got reduced and the formation of metallic cobalt was confirmed. According to Eq. 1, 20 mmol (1.11 mL) of AcH are necessary for the reduction
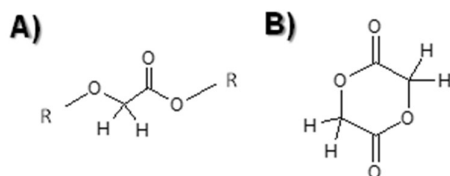
Figure 9. Chemical structure of (A) a segment of the EG-oxidized species and (B) glycolide.

Figure 10. FTIR spectra of EG and samples 5a and 5b.

of 10 mmol of Co^{2+} to Co, leading to 10 mmol (0.87 mL) of diacetyl. Thus, if AcH is generated according to Eq. 1, the amount necessary for the analysis should be easily obtained.

Figure 8 shows the ^{1}H-NMR spectra of the samples along with that of AcH and EG. Spectrum of sample 1 exhibited a singlet peak at 5.26 ppm, in addition to the peaks recored for EG. Sample No. 2 was similar to sample 1 and suggested that heating EG in the presence of water does not undergo any additional chemical reaction or transformation. However, sample No. 3 could not be dissolved evenly in deuterochloroform ($CDCl_3$) for the analysis of EG-oxidized species concentration based on the ratio of integrated intensity of ^{1}H-NMR peak. Similarly, samples 5a and 5b were also could not be dissolved in $CDCl_3$. On the other hand, when metallic Co was introduced into EG, a volatile compound was collected (Figure 8, 4b) but could not be identified-with known profiles.

The proton peak corresponding to aldehyde group is known to appear at 9.79 ppm (AcH, SDBS No. 305)[36] and denoted as A in Figure 8. Not exclusively in the case of aldehyde, but in the cases of proton shielded by the electron cloud in either aldehyde or carboxylate group, the peak appears in the vicinity of 10 ppm.[37] Thus, in the cases where the sample contains AcH, aldehyde compounds or carboxylic acid, peak in the vicinity of 10 ppm should be detected. However, no peak was detected in any of the samples. Thus, the above results confirm that AcH is not generated in the polyol process. Consequently, redox reaction proposed in eq. 1^{14} could not be confirmed in the present case.

ESI-TOFMS analyses of EG prior to and after the reaction were performed. The relative intensity of AcH was only 0.08% when the intensity of the mass equivalent to two EG molecules were set at 100 %. Moreover, the formation of AcH during ESI-TOFMS measurement or the presence of this compound as a contaminant in EG cannot be ruled out. The apparent discrepancies between this work and that were reported previously by Blin et al.[14b] could be explained considering the fact that: i) the experimental setups were different (there is N_2 purging in the present work while water was added first in the reaction system then distilled out) and ii) the reaction conditions were different. As regards the later point, the Co particles were prepared from $Co(OH)_2$ by heterogeneous reaction system in the presence of 3.0 nm sized Pd particles.

From the ^{1}H-NMR spectra of EG shown in Figure 8, it could be deduced that the structure around the hydroxyl group undergoes changes when heated or reacted. This can be due to the change from gauche conformation type to energetically stable anticlinal conformation type. ^{1}H-NMR spectra of the EG
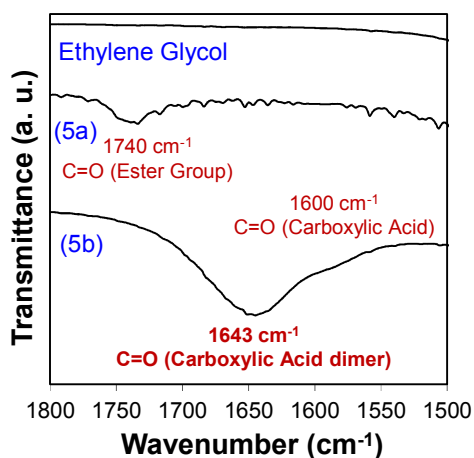
with anticlinal conformation exhibits a chemical shift and corresponding peaks at 3.72 and 3.17 ppm (SDBS No. 2185)[36] have been observed in samples 1, 2, 4a, and 4b as shown in Figure 8. For the EG molecules that were not subjected to any heating, the broad signal at about 2 ppm is attributed to the proton of the hydroxyl group involved in a hydrogen bond for the gauche type conformation (Figure 8, EG, peak a). This was confirmed from the disappearance of the same in the ^{1}H-NMR spectrum of EG obtained in heavy water and shown in inset of Figure 8.

Though the gauche conformation is energetically stable over the anticlinal conformation of EG, transition occurs when EG is subjected to heat[28] and this may have caused the difference in the peak corresponding to hydroxyl group in Figure 8. It should be noted that there is a possibility for the reversal of the conformation from anticlinal to gauche to take place when cooled to R.T. However, since the anticlinal-gauche transition is not directly related to the redox reaction, detailed analysis was not carried out.

In the cases of the spectra of samples 1, 2, 3 and 4a, a singlet peak appeared at 5.26 ppm. This peak appeared only in samples that were either subjected to just heating or where heating is associated with the reduction reaction of Co^{2+} to Co metal. Thus the origin of the peak is considered to be from EG-oxidized species. Since the proton shielding is weak and there is no peak splitting, the singlet peak at 5.26 ppm was assumed to be from the chemical structure shown in Figure 9 (A). Since
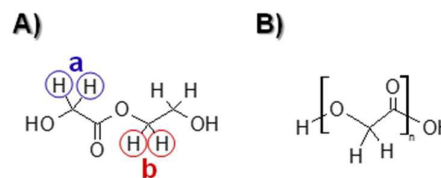
Figure 11. Chemical structures of (A) $C_4H_9O_4$ with (a) and (b) types of protons and (B) polyglycolic acid.
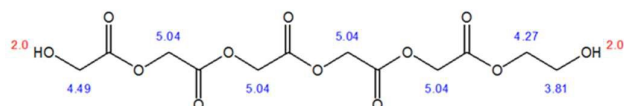
Figure 12. Calculated chemical shifts of glycolic acid oligomer.

the electronegativity of oxygen atom is higher than that of the carbon atom, the shielding becomes lower due to inductive effect in the molecule. And also, coupling does not occur due to the absence of other protons in the vicinity. Consequently, the peak observed should be singlet. Since the glycolide with the structure shown in Figure 9 (B) is also known to exhibit a singlet peak at 4.994 ppm,[38,39] the probability of the EG-oxidized species to have a similar structure is high.

Figure 10 shows the results of the FT-IR spectra of EG and samples 5a and 5b. The sample 5a that contains the oxidized species of EG exhibited a peak at 1740 cm^{-1} that corresponded to the stretching vibration of the C=O in esters.[38] On the other hand, the sample 5b that was obtained from hydrolysing sample 5a, exhibited a strong peak at 1643 cm^{-1} and a weak peak at 1600 cm^{-1}. The above peaks corresponded to vibration modes of C=O in carboxylic acid dimer and carboxylic acid.[40] Thus, the results confirm that the oxidized species of EG generated during the synthesis of metallic cobalt are ester compounds. To analyse the products further, ESI-TOFMS of samples 5a and 5b were carried out. When the peak corresponding to EG dimer was fixed as 100%, 4.6 % of $C_4H_9O_4$ (Figure 11, mes. m/z: 121.0505, calc. m/z: 121.0495) was detected only in sample 5a and not in 5b.

However, $C_4H_9O_4$ is not considered as the main oxidized species of EG. The reason being that, besides the singlet ^{1}H-NMR peak around 5 ppm that corresponds to the proton type (a) shown in Figure 11 (A), a peak corresponding to proton type (b) should also appear. However, such a peak was not recorded in the ^{1}H-NMR spectra (see Figure 8). This discrepancy between ^{1}H-NMR and ESI-TOFMS results may have originated from the large molecular weight of polyglycolic acid shown in Figure 11 (B). The low ionization efficiency of polyglycolic acid may have inhibited the direct detection using ESI-TOFMS.

And also, the chemical transformation, such as the formation of polyglycolic acid in the sample should be considered. The formation of polyglycolic acid within samples 3, 5a, and 5b is supported by the very low solubility of the oxidized species of EG in CDCl$_3$. It has been reported that the solubility of polyglycolic acid becomes low with the increase in their molecular weight.[41]

For reference, the chemical shifts observed in ^{1}H-NMR spectra of polyglycolic acid (n = 5) have been calculated by using ChemDraw Ultra 7.0 and are given in Figure 12. The chemical shift was calculated to be 5.04 ppm as against experimentally observed value of 5.26 ppm. The discrepancy between the values could be due to the non-consideration of interaction during calculations, besides the experimental conditions.
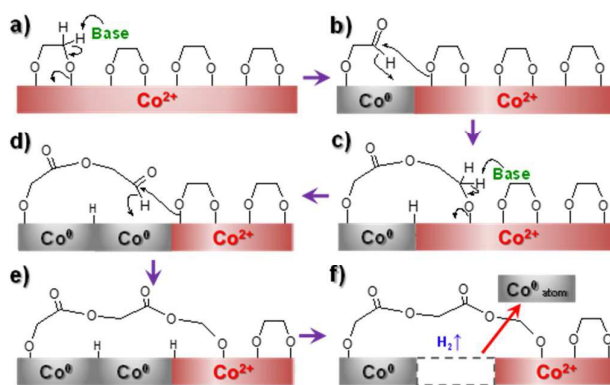
Figure 13. Schematic illustrations of overall redox mechanism in polyol process for Co-EG system. (a) Base attacks proton of Co glycolate. (b) Ester bond is formed through bond exchange. (c) Base attacks proton of neighbouring Co glycolate. (d) Ester bond is formed through bonds exchange. (e) As result of bond exchange, hydrogen atom of the aldehyde group shifts to the Co surface as hydride ion. (f) H$_2$ gas desorbed from the surface and reduced Co^0 atoms dissolves into the solution.

From the above results, the redox reaction in the Co-ethylene glycol system can be summarized as shown in Figure 13. As described in Figure 13 (a), first the base attacks the proton in Co glycolate and the electrons are transferred to Co^{2+} and ethylene glycol get oxidized to aldehyde. Then, the aldehyde undergoes bond exchange with the neighbouring ethylene glycol, and ester is formed as shown in Figure 13 (b). Then, the redox reaction progresses through the repetition of the above two steps as described in Figures 13 (c), (d) and (e). Then, the hydrogen atoms coordinated with Co get detached and evolves as hydrogen gas (Figure 13 (f)). Though the evolution of the gas bubble was visible, its identification was not possible due to low concentration and dilution of the evolved gas by purged nitrogen. On the other hand, the Co^0 atom is released into the liquid medium as shown in Figure 13 (f). This has been confirmed from the fact that a complex composed of two Co^0 atoms has been identified from the ESI-TOFMS spectra of sample 3 ($C_4H_{13}Co_2O_4$, mes. m/z: 242.3453, calc. m/z: 242.9472) as shown in Figure 14.

The formation of Co glycolate becomes a very important intermediate step in Co^{2+} ion reduction; controlling the reactions that follow facilitate the tuning of the size and shape of Co metal particles. Thus, we attempted to synthesize Co metal using Co glycolate as Co source prepared using the recipe given in the experimental section 2.2 with 20 mmol Na metal, and ethylene glycol. The reduction reaction was carried out in the presence of different chemical additives such as sodium
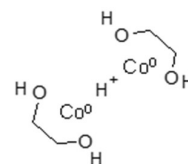
Figure 14. Structural formula of Co^0 complex determined by analysing sample 3 with ESI-TOFMS.
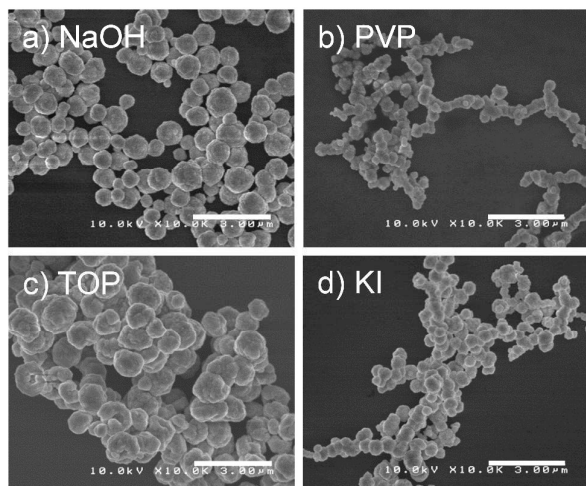
Figure 15. SEM images of Co metal particles synthesized in EG using Co glycolate as Co precursor in the presence of (a) 50 mmol NaOH, (b) 50 mmol NaOH and 27 mmol PVP, (c) 50 mmol NaOH and 10 mmol TPP and (d) 50 mmol NaOH and 10 mmol KI. Scale bar: 3 µm.

hydroxide (NaOH), polyvinylpyrrolidone (PVP), triphenyl phosphine (TPP) and potassium iodate (KI). In contrast to similar experiments carried out using $CoCl_2.6H_2O$ as Co source or Co glycolate, the reduction of Co^{2+} ions was completed in 10 min at 190 °C. SEM images showed in Figure 15 reveal the formation of irregularly shaped Co particles through the aggregation of small particles. The magnetic interaction among the particles is also observed even when surfactant such as PVP was used (Figure 15 (b)). Average sizes of Co particles synthesized using NaOH, PVP, TPP and KI were 790, 340, 970 and 440 nm, respectively. The reason for the difference observed between additives could be due to the superficial adsorption on the Co particle surface.

The above results suggest that the oxidation reaction of ethylene glycol and reduction of Co ion could be explained by the schematic representation given in Figure 13. These findings will have a considerable impact on future understanding of polyol process in synthesizing nanostructures and will pave the way for designed synthesis of metallic and alloy nanoparticles using polyol as well as long chain alcohols.

Conclusions

A detailed investigation of the Co(II)-EG system was undertaken to the reaction mechanism leading to the formation of metallic Co. This implied that the investigation should be carried out not only on the solid phase, but also in the liquid phase, in order to identify the possible Co-containing intermediate phases as well as the oxidation products of EG. From the structural and spectral analyses of the products obtained during the redox reaction in Co-EG system using XRD, NMR, FT-IR and ESI-TOFMS, the following conclusions can be derived. In the case of the reduction reaction, metallic Co is formed via the formation of Co glycolate. The presence of basic ions such as hydroxyl, and acetate ions are indispensable for the formation of monoanion EG^- species, which subsequently facilitates the generation of intermediate cobalt glycolate phase that subsequently undergoes reduction to form metallic Co. This has been experimentally confirmed through the non-reduction of cobalt ions, when $CoCl_2$ was used as the precursor. On the other hand, in the case of the oxidation reaction of EG, the formation of glycolic acid oligomers has been identified. Finally, an overall redox scheme has been proposed to account for all the experimental observations. This study could be widely used for the preparation of metal and alloy nanoparticles using polyols or alcohols.

Acknowledgements

Notes and references

1   W. H. Qi, *Physica B*, 2005, **368**, 46-50.
2   R. A. Van Santen, *Acc. Chem. Res*., 2009, **42**, 57-66.
3   G. Cao and Y. Wang, *Nanostructures and Nanomaterials*, 2nd ed.; World Scientific Publishing Co. Pte. Ltd, USA, 2011.
4   C. Amiens, B. Chaudret, D. Ciuculescu-Pradines, V. Colliere, K. Fajerwerg, P. Fau, M. Kahn, A. Maisonnat, K. Soulantica and K. Philippot, *New J. Chem*., 2013, **37**, 3374-3401.
5   J. L. Cuya Huaman, K. Sato, S. Kurita, T. Matsumoto and B. Jeyadevan, *J. Mater. Chem*., 2011, **21**, 7062-7069.
6   J. L. Cuya Huaman, N. Hironaka, S. Tanaka, K. Shinoda, H. Miyamura and B. Jeyadevan, *CrystEngComm*., 2013, **15**, 729-737.
7   J. L. Cuya Huaman, S. Fukao, K. Shinoda and B. Jeyadevan, *CrystEngComm*., 2011, **13**, 3364-3369.
8   B. Jeyadevan, K. Urakawa, A. Hobo, N. Chinnasamy, K. Shinoda, K. Tohji, D. D. J. Djayaprawira, M. Tsunoda and M. Takahashi, *Jpn. J. Appl. Phys*., 2003, **42**, L350-L352.
9   T. Nakamura, Y. Tsukahara, T. Yamauchi, T. Sakata, H. Mori and Y. Wada, *Chem. Lett*., 2007, **36**, 154-155.
10   B. Jeyadevan, J. L. Cuya, Y. Inoue, K. Shinoda, T. Ito, D. Mott, K. Higashimine, S. Maenosono, T. Matsumoto and H. Miyamura, *RSC Adv*., 2014, **4**, 26667-26672.
11   L. K. Kurihara, G. M. Chow and P. E. Schoen, *Nanostruct. Mater*., 1995, **5**, 607-613.
12   G. Viau, F. Fiévet-Vincent and F. Fiévet, *Solid State Ionics*, 1996, **84**, 259-270.
13   S. Ayyappan, R. S. Gopalan, G. N. Subbanna and C. N. R. Rao, *J. Mater. Res*., 1997, **12**, 398-401.
14   a) F. Fievet, J. P. Lagier, B. Blin, B. Beaudoin and M. Figlarz, *Solid State Ionics*, 1989, **32-33**, 198-205; b) B. Blin, F. Fiévet, D. Beaupère and M. Figlarz, *New J. Chem*., 1989, **13**, 67-72.
15   a) M. Figlarz, F. Fievet and J. P. Lagier, Reduction process of metal-based inorganic precursors in liquid polyols to produce monodisperse metal particles. French Patent 8221483, Dec. 21, 1982. b) Process for reducing metallic compounds using polyols, and metallic powders produced thereby. Europe Patent. 0113281, Dec. 20, 1983. c) Process for the Reduction of Metallic Compounds by Polyols, and Metallic Powders Obtained by This Process. U.S. Patent 4539041, Sep. 3, 1985. d) Menetelmä metal-liyhdisteiden pelkistämiseksi polyoleilla

ja tällä men etelmällä saatu-ja metallijauhe. Finland Patent 74416, Nov. 16, 1985.

16 F. Fievet, J. P. Lagier and M. Figlarz, *MRS Bull.*, 1989, **14**, 29-34.

17 R. J. Joseyphus, K. Shinoda, D. Kodama and B. Jeyadevan, *Mater. Chem. Phys.*, 2010, **123**, 487-493.

18 R. J. Joseyphus, D. Kodama, T. Matsumoto, Y. Sato, B. Jeyadevan and K. Tohji, *J. Magn. Magn. Mater.* 2007, **310**, 2393-2395.

19 D. Kodama, K. Shinoda, K. Sato, Y. Sato, B. Jeyadevan and K. Tohji, *J. Magn. Magn. Mater.,* 2007, **310**, 2396-2398.

20 D. Kodama, K. Shinoda, K. Sato, Y. Konno, R. J. Joseyphus, K. Motomiya, H. Takahashi, T. Matsumoto, Y. Sato, K. Tohji and B. Jeyadevan, *Adv. Mater.*, 2006, **18**, 3154-3159.

21 R. J. Joseyphus, K. Shinoda, Y. Sato, K. Tohji and B. Jeyadevan, *J. Mater. Sci*., 2008, **43**, 2402-2406.

22 S. Ammar, A. Helfen, N. Jouini, F. Fiévet, I. Rosenman, F. Villain, P. Molinie and M. Danot, *J. Mater. Chem.*, 2001, **11**, 186-192.

23 T. Rhadfi, L. Sicard, F. Testard, O. Tache, A. Atlamsani, E. Anxolabehere-Mallart, Y. Le Du, L. Binet and J. Y. Piquemal, *J. Phys. Chem. C*, 2012, **116**, 5516-5523.

24 J. L. Cuya Huaman, K. Tanoue, H. Miyamura, T. Matsumoto, and B. Jeyadevan, *New J. Chem*., 2014, **38**, 3421-3428.

25 K. Nishimura, J. L. Cuya Huaman, H. Miyamura, T. Akiyama, T. Oku and B. Jeyadevan, *Mater. Res. Express*, 2014, **1**, 015032.

26 R. J. Joseyphus, T. Matsumoto, H. Takahashi, D. Kodama, K. Tohji and B. Jeyadevan, *J. Solid State Chem*., 2007, **180**, 3008-3018.

27 J. McMurry and E. E. Simanek, *Fundamentals of Organic Chemistry*, 6th ed. pp. 244. Thomas Brooks/Cole, 2007.

28 T. Matsumoto, K. Takahashi, K. Kitagishi, K. Shinoda, J. L. Cuya Huaman, J.-Y. Piquemal and B. Jeyadevan, *New J. Chem*., 2015, **39**, 5008-5018.

29 N. Chakroune, G. Viau, S. Ammar, N. Jouini, P. Gredin, M. J. Vaulay and F. Fiévet, *New J. Chem*., 2005, **29**, 355-361.

30 N. Hiyama, *Basic Studies on the development of a synthesis process for Plate-shaped FeCo particles*. Master's Thesis, Tohoku University, 2009.

31 F. Bonet, C. Guéry, D. Guyomard, R. H. Urbina, K. Tekaia-Elhsissen and J. M. Tarascon, *Solid State Ionics*, 1999, **126**, 337-348.

32 F. Bonet, C. Guéry, D. Guyomard, R. H. Urbina, K. Tekaia-Elhsissen and J.-M. Tarascon, *Int. J. Inorg. Mater*., 1999, **1**, 47-51.

33 D. Larcher and R. Patrice, *J. Solid State Chem*., 2000, **154,** 405-411.

34 T. Matsumoto, K. Urakawa, R. J. Joseyphus, K. Tohji and B. Jeyadevan, *Electrochemistry*, 2007, **75**, 969-975.

35 K. J. Carroll, J. U. Reveles, M. D. Shultz, S. N. Khanna and E. E. Carpenter, *J. Phys. Chem. C*, **2011**, **115**, 2656-2664.

36 SDBSWeb: http://sdbs.riodb.aist.go.jp (National Institute of Advanced Industrial Science and Technology, Date of access: 2015.07.06

37 Y. Izumi, M. Ogawa, S. Kato, J. Shiokawa and T. Shiba, *Handbook of Instrumental Analysis*, 2nd ed.; Kagakudojin Co. Ltd., Kyoto, 1996, pp. 15-34.

38 C. D. C. Erbetta, R. J. Alves, J. M. Resende, R. F. Freitas and R. G. Sousa, *J. Biomater. Nanobiotechnol*., 2012, **3**, 208-225.

39 B. C. Min, S. H. Kim, S. H. Kim, S. Kwon, H. J. Kim and W. G. Kim, *Bull. Korean Chem. Soc*., 2000, **21**, 635-637.

40 R. M. Silverstein, F. X. Webster and D. J. Kiemle, *Spectroscopic Identification of Organic Compounds, Concomitant use of MS, IR, NMR*, 7th ed.; Wiley, 2007, pp. 126-130.

41 Biodegradable Polymers. Sigma-Aldrich: http://www.sigmaaldrich.com/materials-science/polymer-science/resomer.html.

Graphical abstract:

New Redox reaction mechanism in the formation of Co metal particles using ethyleneglycol-cobalt system is proposed using NMR, ESI-MS, FT-IR and XRD as analytical tools.